

Supplementary Information for

**In-Situ Atomic-Scale Observation of Inhomogeneous Oxide Reduction**

Xiaobo Chen,<sup>a</sup> Dongxiang Wu,<sup>a</sup> Lianfeng Zou,<sup>a</sup> Qiyue Yin,<sup>a</sup> Hanlei Zhang,<sup>a</sup> Dmitri N. Zakharov,<sup>b</sup> Eric A.  
Stach,<sup>c</sup> and Guangwen Zhou<sup>a\*</sup>

<sup>a</sup>Materials Science and Engineering Program & Department of Mechanical Engineering, State University  
of New York at Binghamton, NY 13902, USA

<sup>b</sup>Center for Functional Nanomaterials, Brookhaven National Laboratory, Upton, NY 11973, USA

<sup>c</sup>Department of Materials Science and Engineering, University of Pennsylvania, Philadelphia, PA 19104,  
USA

\*Email: [gzhou@binghamton.edu](mailto:gzhou@binghamton.edu) (G. Zhou)

### Supplementary Note 1. Cu<sub>2</sub>O thin film preparation by oxidation of Cu

Our experiments were performed in a dedicated field-emission environmental TEM (FEI Titan 80-300) equipped with an objective-lens aberration corrector. Thin films of single crystal Cu with  $\sim 500$  Å thickness were grown on NaCl(100) by e-beam evaporation. The Cu films were removed from the substrate by floatation in deionized water, washed, and mounted on a TEM specimen holder. Any native Cu oxide was removed in the TEM by *in situ* annealing the Cu films at  $\sim 600^\circ\text{C}$  and  $1 \times 10^{-3}$  Torr of H<sub>2</sub> flow. Tears and holes with faceted edges developed in the thin film during the annealing (Fig. s1(a)). The Cu film was then oxidized at  $\sim 350^\circ\text{C}$  and  $5 \times 10^{-2}$  Torr of O<sub>2</sub>, which resulted in the growth of a free-standing Cu<sub>2</sub>O thin film along the faceted edges of the Cu film (Fig. s1(b)). Figs. s1(c, d) are diffractograms obtained from the Cu substrate and the Cu<sub>2</sub>O film as marked by the blue dashed squares, respectively, in Fig. s1(b). The diffractograms can be indexed well with Cu<sub>2</sub>O and Cu and their orientation relation can be identified as having cube-on-cube epitaxy, i.e., Cu<sub>2</sub>O(200)//Cu(200) and Cu<sub>2</sub>O[100]//Cu[100].

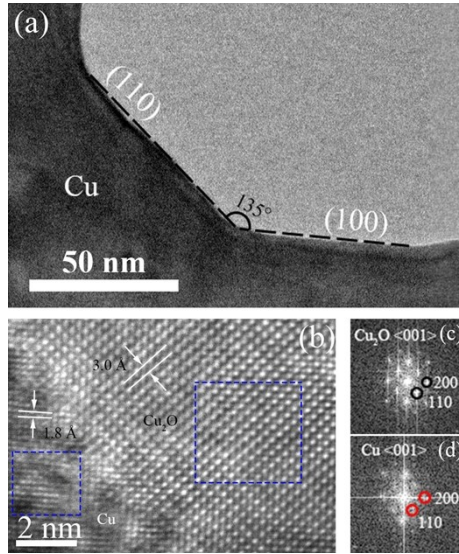


**Fig. s1: Formation of Cu<sub>2</sub>O thin films via the oxidation of Cu.** (a) TEM image of faceted edges by annealing a Cu film at  $600^\circ\text{C}$  and  $1 \times 10^{-3}$  Torr of H<sub>2</sub> gas flow. (b) HRTEM image showing the formation of a Cu<sub>2</sub>O thin film by the oxidation of the Cu film at  $350^\circ\text{C}$  and  $5 \times 10^{-3}$  Torr of O<sub>2</sub> flow. (c, d) diffractograms obtained from the Cu<sub>2</sub>O and Cu regions marked by the blue dashed squares in (b).

## Supplementary Note 2. DFT computational detail

The density-functional theory (DFT) calculations were performed using the Vienna ab-initio simulation package (VASP)<sup>1,2</sup> with the PW91 generalized gradient approximation (GGA) and projector augmented wave (PAW) potentials.<sup>3,4</sup> Our previous works have confirmed that a cutoff energy of 400 eV is sufficient for a well converged system energy.<sup>5,6</sup> The k-point sampling is based on the Monkhorst-Pack grids, and we employed  $4 \times 4 \times 1$  and  $1 \times 4 \times 1$  k-grid for surface and atomic steps, respectively.<sup>2-5</sup>

We modeled the adsorption of Cu adatoms on the Cu<sub>2</sub>O(100) and Cu(100) surface and the diffusion of Cu adatoms on the Cu<sub>2</sub>O(100) surface. The surface atomic steps were modeled by 5 layers with the bottom two layers fixed, while the other three top layers were free to relax until all force components acting on the atoms converged to be within 0.02 eV.<sup>7,8</sup> A vacuum spacing of 12 Å has been used to separate the slabs along the z-axis direction, as confirmed in our previous study.<sup>4-9</sup> The lattice parameters of Cu and Cu<sub>2</sub>O have been calculated to be 3.64 Å and 4.31 Å, respectively, which have been confirmed by our previous study.<sup>10</sup> All the atomic structures were visualized by using the Visualization for Electronic and Structure Analysis (VESTA) program.

## 2.1 Energetics of Cu adatoms on Cu(100) and Cu<sub>2</sub>O(100)

Fig. s2(a) shows one Cu adatom adsorbed at a hollow site of the Cu(100) surface. Fig. s2(b) shows the adsorption of a Cu adatom at a hollow site of the Cu<sub>2</sub>O(100) surface. Our DFT calculations show that the adsorption energies for the Cu adatom at the Cu(100) and Cu<sub>2</sub>O(100) surface are 0.52 eV and Cu<sub>2</sub>O 0.54 eV, respectively.

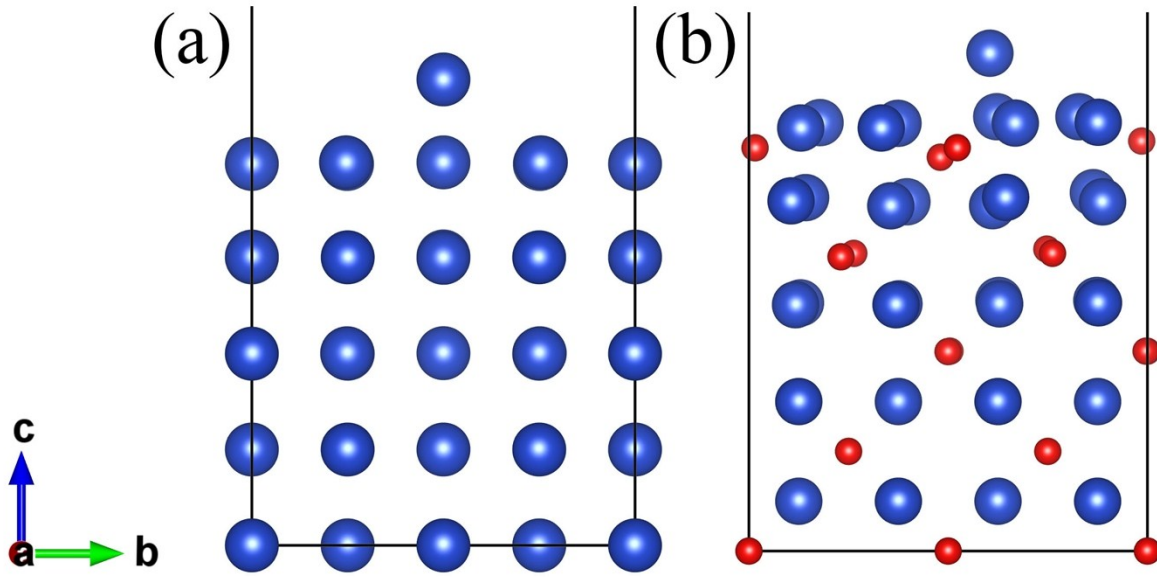


**Fig. s2: DFT modeling of the adsorption of a Cu adatom at a hollow site of the Cu(100) surface (a) and Cu<sub>2</sub>O(100) surface (b). Blue and red spheres represent Cu, and O atoms, respectively.**

## 2.2 Energy barriers for the surface diffusion of Cu adatoms on Cu<sub>2</sub>O(100)

Fig. s3 illustrates the positions of a Cu adatom for the diffusion along the  $[01\bar{1}]$  and  $[011]$  directions of the Cu<sub>2</sub>O(100) surface. Our DFT calculations indicate that the energy barriers for the surface diffusion of a Cu adatom along the  $[01\bar{1}]$  and  $[011]$  directions are 0.52 eV and 0.33 eV, respectively.

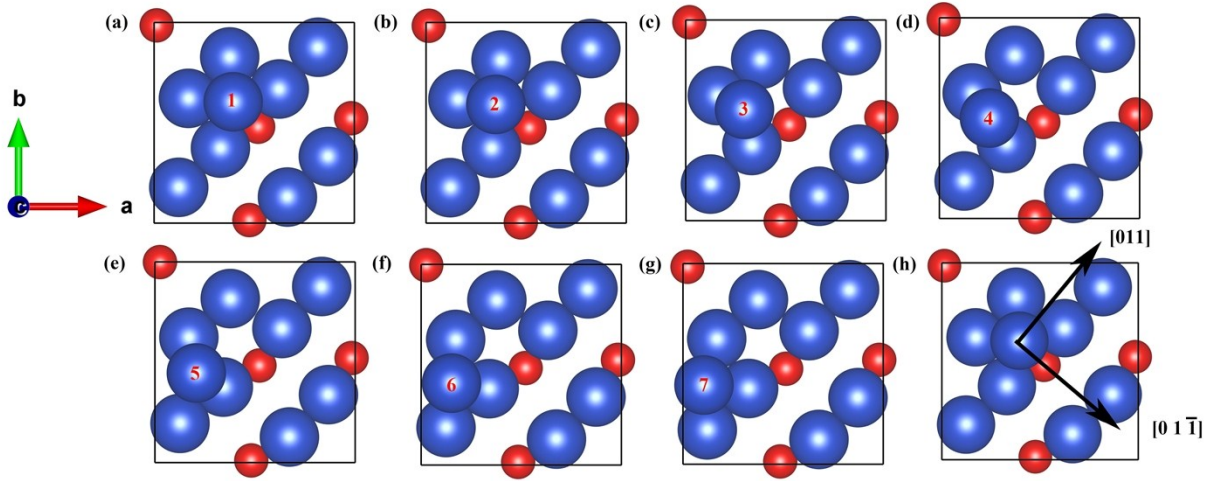


**Fig. s3: DFT modeling of the surface diffusion of Cu adatoms on Cu<sub>2</sub>O(100).** (a-g) snapshot of the Cu atom positions during its diffusion along the  $[110]$  direction. (h)  $[011]$  and  $[01\bar{1}]$  directions for surface diffusion of a Cu adatom on Cu<sub>2</sub>O(100).

### 2.3. DFT calculation for hydrogen adsorption at a perfect $\text{Cu}_2\text{O}(100)$ surface.

Hydrogen adsorption at a perfect  $\text{Cu}_2\text{O}(100)$  surface was also modeled, as shown in Fig. s4. Our DFT calculations indicate that the hydrogen adsorption energy for the perfect  $\text{Cu}_2\text{O}$  surface is  $\sim 1.22$  eV higher than that at surface step sites.

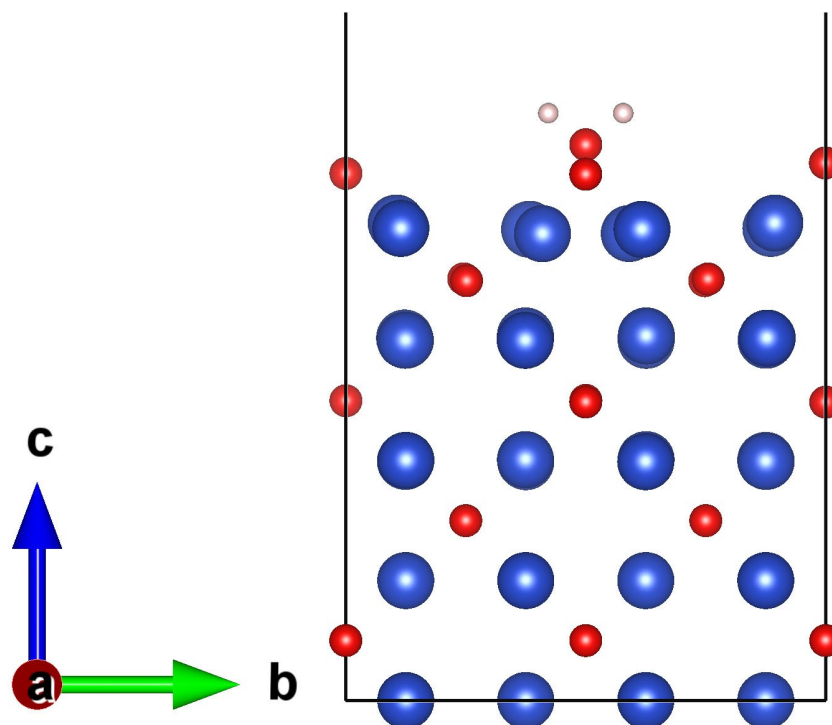


**Fig. s4:** DFT modeling for the hydrogen adsorption at a perfect  $\text{Cu}_2\text{O}(100)$  surface.

## References

- 1 G. Kresse and J. Hafner, *Phys. Rev. B*, 1993, **47**, 558.
- 2 G. Kresse and J. Hafner, *Phys. Rev. B*, 1994, **49**, 14251–14269.
- 3 G. Kresse and J. Furthmüller, *Comput. Mater. Sci.*, 1996, **6**, 15–50.
- 4 G. Kresse, J. Furthmüller and J. Hafner, *Epl*, 1995, **32**, 729–734.
- 5 P. E. Blöchl, *Phys. Rev. B*, 1994, **50**, 17953–17979.
- 6 G. Zhou, L. Luo, L. Li, J. Ciston, E. A. Stach and J. C. Yang, *Phys. Rev. Lett.*, 2012, **109**, 1–5.
- 7 D. Wu, J. Li and G. Zhou, *Surf. Sci.*, 2017, **666**, 28–43.
- 8 W. Shan, Q. Liu, J. Li, N. Cai, W. A. Saidi and G. Zhou, *J. Chem. Phys.*, , DOI:10.1063/1.4972070.
- 9 R. Zhang, B. Wang, L. Ling, H. Liu and W. Huang, *Appl. Surf. Sci.*, 2010, **257**, 1175–1180.
- 10 L. Zou, J. Li, D. Zakharov, E. A. Stach and G. Zhou, *Nat. Commun.*, 2017, **8**, 307.